Vaughan, N. E. & Lenton, T. M. (2012) Interactions between reducing CO_2 emissions, CO_2 removal and solar radiation management ***Phil. Trans. R. Soc. A*** **370**(1974):4343-4364 **doi: 10.1098/rsta.2012.0188** Published 6 August 2012 **http://rsta.royalsocietypublishing.org/content/370/1974/4343**

Interactions between reducing CO_2 emissions, CO_2 removal, and solar radiation management

Naomi E. Vaughan[1] and Timothy M. Lenton[2]

1. School of Environmental Sciences and Tyndall Centre for Climate Change Research, University of East Anglia, Norwich, NR4 7TJ, UK
2. College of Life & Environmental Sciences, University of Exeter, Exeter, EX4 4PS, UK
Corresponding author: n.vaughan@uea.ac.uk

Abstract

We use a simple carbon cycle-climate model to investigate the interactions between a selection of idealised scenarios of mitigated CO_2 emissions, carbon dioxide removal (CDR), and solar radiation management (SRM). Two CO_2 emissions trajectories differ by a 15 year delay in the start of mitigation activity. SRM is modelled as a reduction in incoming solar radiation that fully compensates the radiative forcing due to changes in atmospheric CO_2 concentration. Two CDR scenarios remove 300 PgC by afforestation (added to vegetation and soil) or 1000 PgC by bio-energy with carbon capture and storage (removed from system). Our results show that delaying the start of mitigation activity could be very costly in terms of the CDR activity needed later to limit atmospheric CO_2 concentration (and corresponding global warming) to a given level. Avoiding a 15 year delay in the start of mitigation activity is more effective at reducing atmospheric CO_2 concentrations than all but the maximum type of carbon dioxide removal interventions. The effects of applying SRM and CDR together are additive, and this shows most clearly for atmospheric CO_2 concentration. SRM causes a significant reduction in atmospheric CO_2 concentration due to increased carbon storage by the terrestrial biosphere, especially soils. However, SRM has to be maintained for many centuries to avoid rapid increases in temperature and corresponding increases in atmospheric CO_2 concentration, due to loss of carbon from the land.

Vaughan, N. E. & Lenton, T. M. (2012) Interactions between reducing CO_2 emissions, CO_2 removal and solar radiation management ***Phil. Trans. R. Soc. A*** **370**(1974):4343-4364 **doi: 10.1098/rsta.2012.0188** Published 6 August 2012 **http://rsta.royalsocietypublishing.org/content/370/1974/4343**

1 Introduction

The dominant policy approach to limiting future climate change is to reduce anthropogenic emissions of greenhouse gases and other radiative forcing agents. However, in recent years there has been a resurgence of interest in the potential to complement these mitigation approaches with 'geoengineering' methods (Crutzen, 2006). Geoengineering can be subdivided into active 'carbon dioxide removal' (CDR) from the atmosphere, and reducing the absorption of incoming sunlight – termed 'solar radiation management' (SRM). Existing work has sought to compare the effectiveness of different geoengineering methods, against a background of mitigation (Lenton & Vaughan, 2009; Royal Society, 2009; Vaughan & Lenton, 2011). However, relatively little attention has been directed at how the different approaches would interact with one another, were they deployed together. In particular, are they synergistic (doing more of one thing means you have to do less of another) or antagonistic, when it comes to their effects on global temperature, atmospheric CO_2 concentration, and other aspects of the carbon cycle? Furthermore, can the prospect of geoengineering really 'buy time', and reduce the impact of delays in starting substantive global emissions reductions? In this paper we address these questions using a simple carbon cycle-climate model.

Any discussion of the possible use of geoengineering requires an assumption to be made about the future trajectory of anthropogenic CO_2 emissions (from fossil fuel combustion and land use change). Land use change emissions remained fairly constant (at 1.47 ± 0.05 PgC yr^{-1}) over the last ten years of available data (1996-2005) (Houghton, 2008). Meanwhile fossil fuel emissions increased by 20% over that same period (1996-2005) (Boden *et al.*, 2011). Despite the recent global economic downturn, emissions from fossil fuel and cement production since 2005 have exceeded 8 PgC yr^{-1} (Table 1). The choice of future fossil fuel emission trajectory has a significant impact on the magnitude of excess CO_2 in the atmosphere and therefore the amount of global warming and extent of future climate change. Peak temperatures respond to the cumulative anthropogenic emissions (Lenton, 2000; Allen *et al.*, 2009; Matthews *et al.*, 2009). When considering the possible use of geoengineering as a complement to mitigating emissions it is important to consider the transient response of the climate system (Wigley, 2006).

Year	Model PgC	Actual PgC	Difference model-actual	Reference
2000	6.750	6. 750	0	
2001	6.916	6.916	0	
2002	6.981	6.981	0	
2003	7.397	7.397	0	
2004	7.782	7.782	0	Boden *et al.*, 2011
2005	8.086	8.086	0	
2006	8.225	8.350	0.125	
2007	8.365	8.543	0.178	
2008	8.509	8.749	0.240	
2009	8.654	8.626	-0.028	Boden & Blasing (2011)
2010	8.803	9.139	0.336	

Table 1 Comparison of modelled fossil fuel and cement production emissions with actual emission estimates for 2000 to 2010.

Vaughan, N. E. & Lenton, T. M. (2012) Interactions between reducing CO_2 emissions, CO_2 removal and solar radiation management ***Phil. Trans. R. Soc. A*** **370**(1974):4343-4364 **doi: 10.1098/rsta.2012.0188** Published 6 August 2012 **http://rsta.royalsocietypublishing.org/content/370/1974/4343**

Most equilibrium response studies of geoengineering make no explicit assumption about an emissions trajectory, instead defining atmospheric CO_2 concentrations such as double pre-industrial (e.g. Govindasamy & Caldeira, 2000; Caldeira & Wood, 2008; Bala *et al.*, 2008) or quadruple pre-industrial (e.g. Govindasamy *et al.*, 2003, Lunt *et al.*, 2008, Irvine *et al.,* 2010). Some transient response studies assume one mitigation scenario, Matthews & Caldeira (2007) and Matthews *et al*. (2009) use SRES A2 and Ricke *et al.* (2009) use SRES A1B, both of which are high-end, i.e. limited climate policy scenarios (Nakicenovic *et al.*, 2000). All these geoengineering studies investigate various impacts of SRM alone, with varying complexities of models. Moore *et al.* (2010) consider the impact on sea level rise of both SRM and CDR (but not in combination) in the context of three Representative Concentration Pathways (RCPs) (Moss *et al.*, 2010). Wigley (2006) investigated three emission pathways; no climate policy, 450 ppm stabilisation and an overshoot (530 ppm peak, returning to 450 ppm) and their interaction with varying levels of SRM intervention (approximating radiative forcing impact of Mt Pinatubo, i.e. periodic injections of sulphate aerosols into the stratosphere). Goes *et al.* (2011) use an integrated assessment model to investigate the economic impacts of SRM (by stratospheric aerosol injection) with industrial CO_2 emissions determined endogenously by their economic model. Matthews & Caldeira (2007) modelled a transient response to SRM geoengineering (assuming a complete compensation of the radiative forcing due to atmospheric CO_2 concentrations in excess of pre-industrial levels). They found that terrestrial and ocean carbon sinks (combined) became stronger in response to the imposed global cooling, resulting in lower atmospheric CO_2 levels in the geoengineered model runs. This artificial strengthening persisted in the model only as long as the SRM was in place (Matthews & Caldeira, 2007). Matthews *et al.* (2009) investigated the effect of SRM on ocean chemistry and included model runs with no land-atmosphere exchange of CO_2 once SRM commenced. They show that the sign and magnitude of the effect of SRM on ocean chemistry are dependent on the response of the terrestrial biosphere.

We use a simple model (Lenton, 2000; Lenton & Huntingford, 2003) to investigate the individual and combined impacts of CDR and SRM applied to two different future emissions profiles. The use of a simple model, although overlooking a range of important forcings factors and feedbacks, allows a first-order examination of the interactions between these different interventions in the carbon cycle-climate system.

2 Methods

We use a box model of the carbon cycle (Figure 1) coupled to a grey-atmosphere approximation of the Earth's radiation budget (Lenton, 2000), which gives a mid-range climate sensitivity of ≈3 °C global warming for a doubling of atmospheric CO_2 (Figure 2). Figure 1 shows schematically how carbon is transferred between the atmosphere, vegetation and soil. In the model the rate of change of the vegetation carbon reservoir, C_v, (before including land use change processes), is given by:

$$\frac{dC_v}{dt} = P(CO_2, T) - R_p(C_v, T) - L(C_v) \qquad (1)$$

where P is gross photosynthesis (i.e. the transfer of carbon from the atmosphere to vegetation), CO_2 is atmospheric CO_2 concentration, T is global surface temperature, R_p is plant respiration comprised of growth and maintenance respiration (i.e. transfer of carbon from vegetation to atmosphere) and L is litter fall and

plant death (i.e. the transfer of carbon from vegetation to soil, see Figure 1). The balance of photosynthesis and respiration, P - R_p, gives the net primary productivity (NPP). The rate of change of the soil carbon reservoir, C_s, is given by:

$$\frac{dC_s}{dt} = L(C_v) - R_s(C_s, T) \qquad (2)$$

where R_s is soil respiration. Photosynthesis, P, plant respiration, R_p and soil respiration, R_s are all a function of temperature, but only photosynthesis is also a function of CO_2 concentration (see Lenton, 2000 and Lenton & Huntingford, 2003 for further details). These dependences are key to understanding the results in Section 3 for the changes in the vegetation and soil carbon reservoir and the land carbon flux (Figures 6, 8 & 10).

The model is forced with estimates of CO_2 emissions from historical land use change (Houghton, 2008), fossil fuel combustion and cement production (Boden *et al.*, 2011) for the period 1800 to 2000 (Figure 3a, Figure 4). Data for emissions from land use change for the period 1800 to 1850 are estimated based on UN population estimates (1800 = 0.98 billion, 1850 = 1.26 billion), giving a linear increase from 0.39 PgC in 1800 to 0.501 PgC in1850 (UNPD, 1999; Houghton 2008). Land use change emissions after the year 2005 are an idealised profile where 100 PgC is emitted with an exponential decay rate, k=0.0141 (Figure 3a). Carbon emitted from land use change is all removed from the vegetation reservoir (Figure 1) and acts to reduce equilibrium vegetation carbon storage by a fraction k_D = 0.27 of the cumulative land use change emission, which accounts for the fact that some land use change is permanent deforestation (Lenton, 2000).

For CO_2 emissions from fossil fuel combustion and cement production, after the year 2005, we use a conceptual model of the emissions trajectory (based on Vaughan *et al.*, 2009). We assume a growth rate of emissions of 1.7 % yr^{-1} until mitigation activity commences in a defined start year, T_s. At this time the rate of change of emissions changes linearly over 40 years to -1.7 % yr^{-1}. In a notable modification to our previous work (Vaughan *et al.*, 2009), this shrinkage of emissions at -1.7 % yr^{-1} is then maintained until emissions are negligible. The growth rate of emissions is based on a 25 year average of emissions growth rate (1981-2005) from the latest data (Boden *et al.*, 2011). This choice of a long term trend causes the modelled emissions (Table 1) to be below recent estimates (Boden *et al.*, 2011; Boden & Blasing, 2011), and is lower than used by others (e.g. Anderson & Bows, 2008). However, we argue that when projecting several decades into the future, it is appropriate to use a longer term average of past emissions growth. Here we use two different values for the start of mitigation activity, T_s=2015 and T_s=2030 (Table 2), the resulting profiles are shown in Figure 3a (Figure 4). The 15 year delay in starting mitigation activity ultimately leads to a difference in peak global temperatures of 0.8 °C and in peak atmospheric CO_2 concentration of 112 ppm.

Vaughan, N. E. & Lenton, T. M. (2012) Interactions between reducing CO_2 emissions, CO_2 removal and solar radiation management ***Phil. Trans. R. Soc. A*** **370**(1974):4343-4364 **doi: 10.1098/rsta.2012.0188** Published 6 August 2012 **http://rsta.royalsocietypublishing.org/content/370/1974/4343**

Scenario	Description	Reference
s2015	Start time of mitigation activity, T_s = 2015	Vaughan *et al.*,2009
s2030	Start time of mitigation activity, T_s = 2030	
aff	Afforestation	Lenton, 2010
becs	Biomass Energy with Capture & Storage (BECS)	
s2030srm2015	SRM intervention begins in 2015	
s2030srm2100	SRM intervention begins in 2100	This paper (Figure 5)
s2030srm21002400	SRM intervention begins in 2100 and stops in 2400	
s2015aff	T_s = 2015 and afforestation	This paper (Figure 7)
s2015becs	T_s = 2015 and BECS	
s2030aff	T_s = 2030 and afforestation	
s2030becs	T_s = 2030 and BECS	
s2030srm21002400aff	T_s=2030, SRM begins in 2100 and stops in 2400 and afforestation	This paper (Figure 9)
s2030srm21002400becs	T_s=2030, SRM begins in 2100 and stops in 2400 and BECS	

Table 2 Scenario nomenclature and description

For carbon dioxide removal (CDR) interventions we use two idealised profiles of CDR from previously published work (Lenton, 2010); afforestation (aff) and bio-energy with carbon storage (becs) (Table 2, Figure 3b). These interventions are idealised by a Gaussian curve centred on year 2100. Afforestation removes a total of 300 PgC and BECS removes a total of 1000 PgC. A removal of 0.24 PgC yr^{-1} occurs in both cases in 2010. The maximum removal of CO_2 occurs in 2100, at 3.0 PgC yr^{-1} for afforestation and 12.5 PgC yr^{-1} for BECS. The afforestation is an upper limit scenario based on more detailed studies (van Minnen *et al*, 2008) which reverses and somewhat exceeds historical and future emissions from land use change on the grounds that managed forests can store more carbon than natural ones. The BECS scenario is considered a maximum level of CDR constrained by the geological storage capacity for CO_2.

For the solar radiation management (SRM) interventions, the scenarios differ in start time and duration (Table 2). We model SRM intervention as a reduction in incoming solar radiation that fully compensates the radiative forcing due to changes in atmospheric CO_2 concentration. Equilibrium response studies, where a dictated future climate (double or quadruple pre-industrial CO_2 concentration) is compared to a pre-industrial climate, impose a fixed percentage reduction to the solar radiation flux (e.g. Govindasamy & Caldeira, 2000; Lunt *et al.*, 2008). Mathews & Caldeira (2007) and Matthews *et al.* (2009) work with a transient response and as such also require, as we do, an ever changing magnitude of SRM in order to maintain pre-industrial temperatures. Matthews & Caldeira (2007) and Matthews *et al.* (2009) apply a factor to the radiative forcing in the UVic model which is specified as the natural logarithm of the modelled atmospheric CO_2 concentration compared to a reference atmospheric CO_2 concentration. Our approach is necessarily different because our model uses a grey atmosphere approximation to calculate the changes in radiative forcing and temperature resulting from changes in atmospheric CO_2 concentration. We note that in reality, cancellation of the radiative forcing from CO_2 and other anthropogenic forcing agents would not be perfect.

Vaughan, N. E. & Lenton, T. M. (2012) Interactions between reducing CO_2 emissions, CO_2 removal and solar radiation management ***Phil. Trans. R. Soc. A*** **370**(1974):4343-4364 **doi: 10.1098/rsta.2012.0188** Published 6 August 2012 **http://rsta.royalsocietypublishing.org/content/370/1974/4343**

In our model the net downward flux of radiation (F_d) absorbed at the planet's surface is given by:

$$F_d = \frac{(1-A)S}{4}\left(1+\frac{3}{4}\tau\right) \quad (3)$$

where A is the (fixed) surface albedo (A = 0.225), S is the incoming solar flux at the top of the atmosphere (S =1368 W m^{-2}) and τ is the (equivalent grey) vertical opacity of the greenhouse atmosphere, which depends on the concentrations of CO_2, $H_2O_{(g)}$ and CH_4. The opacity of each gas is assumed to be independent of the others (Lenton, 2000):

$$\tau = \tau(\mathrm{CO_2}) + \tau(\mathrm{H_2O}) + \tau(\mathrm{CH_4}) \quad (4)$$

We approximate SRM intervention by modifying the incoming solar flux (S) to entirely compensate the changes to atmospheric CO_2 concentration. For SRM to maintain a pre-industrial temperature, then F_d must be held constant. As albedo (A) is constant, this can be achieved by keeping the following constant;

$$k_{srm} = S\left(1+\frac{3}{4}\tau(\mathrm{CO_2})+\frac{3}{4}\tau(\mathrm{H_2O})+\frac{3}{4}\tau(\mathrm{CH_4})\right) \quad (5)$$

We hold atmospheric methane concentration (CH_4) constant at the preindustrial value of 650 ppb, so $\tau(CH_4)$ is also constant, $\tau(CH_4)$ = 0.0231. Furthermore, because the concentration of water vapour and hence its opacity, τ (H_2O) depends only on temperature, and we are aiming to hold that constant, we can assume a constant $\tau(H_2O)$ = 0.4178. The variable opacity of CO_2 is given by:

$$\tau(\mathrm{CO_2}) = 1.73(\mathrm{CO_2})^{0.263} \quad (6)$$

Using the pre-industrial atmospheric concentration of CO_2 (280 ppm) and (5) we find k_{srm} = 2026.8 W m^{-2}. The required SRM intervention to maintain a constant pre-industrial temperature is then given by:

$$S = \frac{k_{srm}}{\left(1.3307+\frac{3}{4}\tau(\mathrm{CO_2})\right)} \quad (7)$$

The continually changing magnitude of SRM is illustrated in Figure 3c and Figure 9c.

Having outlined the mechanisms by which we model future CO_2 emissions, CDR and SRM interventions (summarised in Table 2), in the following section we investigate the impact of SRM intervention alone (Section 3.1), CDR intervention alone (Section 3.2), and the combined use of SRM and CDR (Section 3.3).

Vaughan, N. E. & Lenton, T. M. (2012) Interactions between reducing CO_2 emissions, CO_2 removal and solar radiation management ***Phil. Trans. R. Soc. A*** **370**(1974):4343-4364 **doi: 10.1098/rsta.2012.0188** Published 6 August 2012 **http://rsta.royalsocietypublishing.org/content/370/1974/4343**

3 Results

3.1 Solar Radiation Management

Our SRM experiments are designed such that the global mean temperature change above pre-industrial is rapidly reduced toward zero after commencing the SRM intervention (Figure 5a), with a timescale set by the heat capacity in the model. For s2030srm2015, global warming is reduced from 1.2 °C in 2015 to 0.1 °C in 2040 and 0.01 °C in 2070. For s2030srm2100, global warming is reduced from 3.3 °C in 2100 to 0.3 °C in 2124 and 0.03 °C in 2150. For s2030srm2100, the peak magnitude of SRM intervention is a 2.5 % reduction in incoming solar radiation in the first decade of application. A unique feature of s2030srm2015 is that because anthropogenic CO_2 emissions are still increasing (Figure 3a), the magnitude of SRM intervention increases from 1.0 % reduction in incoming solar radiation in the first year to 2.5 % in 2125 (Figure 3c). These first two scenarios assume a permanent maintenance of the SRM intervention; by the year 3000 a reduction of incoming solar radiation of 1.4 % is still required because the atmospheric CO_2 concentration of 460 ppm is 180 ppm above pre-industrial (Figure 5b). The final SRM scenario demonstrates that if the SRM intervention ceases (s2030srm21002400), the temperature returns to what it would have been without any SRM intervention (s2030), as shown previously with a more complex model (Matthews & Caldeira, 2007).

An interesting feature of the application of the SRM intervention is that it causes a reduction in atmospheric CO_2 concentration (Figure 5b). The maximum drawdown is 74 ppm in 2185 (in scenario s2030srm2015), declining to 49 ppm in 2400 and 38 ppm in 3000. When SRM is stopped in 2400 (in scenario srm21002400), the atmospheric CO_2 concentration rises again towards the concentration level of the no SRM scenario (by 2600 the difference between the two is 4 ppm). The reduction in atmospheric CO_2 caused by SRM intervention is due primarily to the response of the land carbon cycle. Figure 6 shows the transient response of SRM interventions on the vegetation and soil carbon reservoirs (see Figure 1) and the land and ocean sinks.

To understand what is going on it is worth first noting what happens in the absence of SRM (scenario s2030). The vegetation carbon reservoir, C_v (Figure 6a), increases slightly over the historical period (1800 to 2000) by 30 PgC, as the net result of vegetation loss by deforestation (totalling 170 PgC over this period; Houghton, 2008) counteracted by the positive response of vegetation to increasing CO_2 concentration, together with some re-growth. Without any SRM intervention, the C_v continues to increase reaching 730 PgC in 2140, a result of CO_2 fertilisation, beneficial effects of warming, and the reduction in deforestation assumed to take place after year 2000 (from 1.4 PgC yr^{-1} in 2000 to 0.36 PgC yr^{-1} in 2100) (see Section 2). After 2140, C_v decreases over the following centuries, stabilising at ≈650 PgC, as a consequence of declining CO_2. Meanwhile, the soil carbon reservoir, C_s (Figure 6b), shows a decrease over the historical period (1800 to 2000) of 40 PgC due to land use change and a loss of soil carbon due to increased soil respiration driven by rising temperatures (see Section 2). The decline is then reversed with an increase peaking at just over the pre-industrial 1500 PgC in 2100 then declining gradually to ≈1480 PgC by 2500. This post-2000 trend follows the pattern but not the magnitude of changes in C_v (Figure 6a).

The implementation of SRM reduces the storage of carbon in the vegetation reservoir, C_v (Figure 6a). This is because the atmospheric CO_2 concentration is lowered (Figure 5b) and photosynthesis, i.e. the fixation of carbon from the atmosphere to vegetation, is dependent on CO_2 concentration (Equation 1). Interestingly,

SRM implementation lowers C_v more than the alternative mitigation scenario (s2015) (Figure 6a), despite the atmospheric CO_2 concentration being higher in s2030srm2100 than in s2015 (Figure 5b). This is because global warming enhances net primary productivity (the result of competing temperature effects on photosynthesis and plant respiration; Equation 1) (Lenton, 2000). Hence in s2030srm2100, cooling of 2.7 °C to 2 °C relative to s2015 (Figure 5a), lowers carbon fixation and C_v (Figure 6a). When SRM is stopped, the resulting rises in temperature and CO_2 increase net primary production and C_v.

The soil carbon reservoir, C_s (Figure 6b), responds to SRM with the opposite sign and greater magnitude than the vegetation carbon reservoir. With the advent of SRM, C_s increases, peaking at ≈ 1700 PgC in 2180 and stabilising at ≈1580 PgC by 2600. This is because cooling due to SRM reduces temperature-driven, heterotrophic respiratory losses of carbon from soil (Equation 2), which is the key mechanism by which carbon is transferred from the soil to the atmosphere (Figure 1). The effect of continued SRM intervention (s2030srm2015, s2030srm2100) is the additional storage of ≈100 PgC in the soil carbon reservoir, which is counteracted by a loss of ≈70 PgC from the vegetation carbon reservoir, C_v. The net effect is an additional land carbon storage of ≈30 PgC by year 3000. If SRM interventions are stopped, as in s2030srm21002400, the increase in temperature (Figure 5a) causes an increase in soil respiration and the release of ≈100 PgC from C_s (Figure 6b).

The net effect of the changes to vegetation and soil carbon reservoirs can also be expressed in terms of the annual land carbon sink (Figure 6c), where positive values indicate annual net flux of carbon from the atmosphere to the land. Figure 6c shows the increase in this natural carbon sink in response to the elevated atmospheric CO_2 concentration (scenario s2030), peaking in 2042 at 3.7 PgC yr^{-1}. The sink of carbon becomes a slight source from 2135 onwards, reaching a maximum source flux of 0.26 PgC yr^{-1} in ≈2270. With the application of SRM in 2015, the peak land carbon sink is higher (4.3 PgC yr^{-1}) and the later source is stronger (0.58 PgC yr^{-1} in ≈2260). Applying SRM later (s2030srm2100) causes a second peak in the land carbon sink in 2112, at 2.9 PgC yr^{-1}. This second peak occurs as the reduction in global temperature takes effect (Figure 5a). Ceasing SRM intervention in 2400 causes a distinct release of carbon from the land to the atmosphere, which correlates with the rapid increase in temperature (Figure 5a), and is due to loss of carbon from soil (117 PgC by 2500) (Figure 6b) dominating addition of carbon to vegetation (74 PgC by 2500) (Figure 6a).

The impact of SRM intervention on the ocean sink is smaller than on the land sink (Figure 6d). Commencing SRM in 2015 increases the ocean sink from a peak of 4.2 PgC yr^{-1} in 2079 (s2030) to a peak of 4.6 PgC yr^{-1} in 2075 (s2030srm2015). Starting SRM in 2100 causes a short, sharp peak in the ocean sink in 2100, which rapidly decays back to the same size as in the s2030 scenario. The termination of SRM in 2400 causes a short lived weakening of the sink as CO_2 is out-gassed from the surface ocean. At no point in any of these model runs does the ocean become a source of carbon to the atmosphere. The response of the model ocean sink is driven by the temperature and CO_2 dependence of carbonate chemistry in surface waters (Lenton, 2000).

3.2 Carbon Dioxide Removal

We investigate two scenarios of carbon dioxide removal with maximum removal centred on 2100. The afforestation scenario removes a total of 300 PgC from the atmosphere and adds this to vegetation (C_v), from where much is transferred to soil, and equilibrium vegetation carbon storage is increased by a fraction

k_D = 0.27 of the cumulative addition (the opposite of the effects of deforestation). The Bio-Energy with Carbon Storage (BECS) scenario removes a total of 1000 PgC from the system entirely (see Figure 1) (Lenton, 2010). These CDR scenarios are each applied to two different mitigation scenarios; s2030 (black solid) and s2015 (grey dashed) (Figures 7 & 8). Afforestation lowers the peak in global temperature by 0.6 °C and temperature in year 3000 by 0.4 °C, whilst BECS lowers the peak by 1.2 °C and the eventual warming by 1.2 °C in year 3000, compared to the s2030 mitigation scenario (Figure 7a). These reductions in temperature are paralleled by similar magnitude reductions in atmospheric CO_2 concentration (Figure 7b). Afforestation lowers the peak in atmospheric CO_2 concentration by 80 ppm and the concentration in year 3000 by 47 ppm, whilst BECS lowers the peak by 148 ppm and the year 3000 concentration by 122 ppm (Figure 7b). Notably the rate of change of temperature caused by the BECS scenario is significantly greater than the no CDR or afforestation scenarios, and this is important when considering adaptation of ecosystems and human systems. CDR reduces cumulative anthropogenic emissions, leading to less CO_2 accumulating in the atmosphere (Figure 7b), hence less global temperature change (Figure 7a).

Contrasting the s2015 and s2030aff cases shows that starting CO_2 emissions reductions in 2015 is more effective at reducing atmospheric CO_2 concentration and global temperature change (438 ppm, 1.76 °C in year 3000) than starting CO_2 emissions reductions in 2030 and applying a large scale programme of afforestation (452 ppm, 1.88 °C in year 3000). Starting mitigation in 2015 and applying the afforestation scenario (s2015aff) is nearly as effective in the long term as a 15 year delay in mitigation combined with the BECS scenario (s30becs). A combination of starting mitigation in 2015 and undertaking intensive CDR, such as through BECS (s2015becs), can reduce atmospheric CO_2 concentration and global temperature change to near pre-industrial levels, at 333 ppm and 0.67 °C in year 3000 respectively, however this pathway still includes a peak in temperature of 2.1 °C (Figure 7a). A final interesting feature of the BECS scenarios is the impact of a period of net anthropogenic carbon dioxide removal that lasts roughly a century; from 2070 to 2164 inclusive (95 years) for s2015becs and from 2082 to 2152 inclusive (71 years) for s2030becs (Figure 3b). This gives a clear dip in global warming at around 2160 (in 2165 for s2015becs and in 2170 for s2030becs) and in CO_2 concentrations (in 2152 for s2015becs and in 2157 for s2030bec).

The impact of CDR on the land and ocean carbon cycles is illustrated in Figure 8. As expected, when CO_2 is removed from the atmosphere permanently, as in the BECS scenario, the amount of carbon in the vegetation and soil are lower than in the no CDR cases (Figures 8a & 8b). This is because photosynthesis depends on atmospheric CO_2 concentration (Section 2, Equation 1). However, with afforestation, the CO_2 is removed from the atmosphere and placed in the vegetation carbon reservoir, C_v, from where much is transferred to soil (Figure 1). This leads to an increase in the vegetation carbon reservoir of ≈75 PgC (Figure 8a) and an increase in the soil carbon reservoir of about ≈230 PgC (Figure 8b).

The impact of CDR interventions on the land sink is most prominent with the s2015becs scenario; the hundred year period of 'negative emissions' (i.e. net carbon dioxide removal) (Figure 3b) causes the land to respond by becoming a strong source of CO_2 (3.2 PgC yr^{-1} in 2117), driven by the rapid reduction in atmospheric CO_2 concentration (Figure 7b). The negative emissions in the s2015becs scenario are such that there is a reduction of the ocean sink to <0.1 PgC yr^{-1} by 2130, recovering slightly to 0.3 PgC yr^{-1} by 2200 (Figure 8d). In the s2030becs scenario the ocean sink is weakened to only 1.1 PgC yr^{-1} in 2140 compared to a sink of 3.8 PgC yr^{-1} in the same year in the no CDR scenario (s2030). The ocean sink then recovers slightly before returning to a steady decay. This feature is traceable in the land sink, global temperatures and

atmospheric CO_2 (Figures 7 & 8), and is caused by the severity and rapidity of the hundred year period of negative emissions.

3.3 Combined SRM and CDR interventions

Having considered the individual impacts, albeit at different magnitudes, of the two types of geoengineering, SRM and CDR, here we combine the interventions and apply them to the s2030 scenario. In Figures 9 & 10 the earlier mitigation scenario (s2015) is also shown for comparison. In the two geoengineered scenarios, SRM starts in 2100 and stops in 2400 (s2030srm21002400) and either afforestation (s2030srm21002400aff) or BECS (s2030srm21002400becs) are applied. Figure 9 shows the impact of these combined geoengineering interventions on global temperature and atmospheric CO_2 concentration. The way we have implemented SRM dictates that global temperatures are returned to pre-industrial levels. When the SRM is stopped, global temperature rises to the level of the corresponding mitigation (s2030) or mitigation-plus-CDR scenarios (s2030aff or s2030becs). This is in keeping with the results shown in Figure 5 combined with the lower atmospheric CO_2 concentrations caused by CDR (Figure 7). What is not initially obvious is the range in magnitude of SRM required to cause this result (Figure 9). Figure 9c shows the changes to the incoming solar radiation flux that are implemented to achieve Figure 9a.

The combined SRM & CDR approaches are additive, and this shows most clearly for atmospheric CO_2 concentration in Figure 9b. The CDR interventions lower atmospheric CO_2, by the same amount as previously (Figure 7), but the SRM temperature reduction lowers CO_2 concentration further for the period 2100 to 2400. The mechanism is as described in detail in Section 3.1. Figure 10 explores further the ways in which these global temperature changes and atmospheric CO_2 concentration are reached, showing the effects of the combined geoengineering interventions on vegetation and soil carbon reservoirs and the land and ocean carbon sinks. Again, the effects are additive, for example, the changes to the vegetation carbon reservoir, C_v, for the s2030srm21002400aff scenario follow the s2030aff scenario but with a lower peak in C_v (Figures 8a & 10a), because the SRM intervention has lowered the amount of carbon stored in the vegetation by suppressing the positive effect on net primary productivity of moderate warming (Section 3.1). The additive pattern is also evident in the peak in soil carbon reservoir, C_s around 2200, where the increase of ≈200 PgC due to SRM-induced cooling (Figure 6b) combines with the increase of ≈200 PgC due to afforestation (Figure 8b), to increase C_s by ≈400PgC when SRM and afforestation are both implementation in our model (Figure 10b). The long term size of C_s is the same as in Figure 8b because the SRM intervention is stopped in 2400.

The land sink and ocean sink responses to combined interventions are more complex (Figures 10c & 10d). The s2030srm21002400becs scenario causes a much smaller source of carbon due to the hundred year period of negative emissions compared to the s2030becs scenario (Figures 10c & 8c). The double peak in land sink magnitude in Figure 6c caused by the start of SRM in 2100 is also evident here in the s2030srm21002400aff scenario, where the start of the SRM in 2100 lowers global temperatures, thus impeding soil respiration (Section 3.1). In the geoengineered cases, the land sink becomes a land source (Figure 10c) in 2400 as the SRM intervention is stopped and global temperatures rise (Figure 9a). In the combined cases this source is weaker because the change in global temperature is less due to the CDR having removed CO_2 from the atmosphere (Figure 9). In Figure 10d the ocean sink response is also additive, a comparison with Figure 6d and Figure 8d shows the same trends, with the rapid responses by ocean to

the sudden changes in global temperature in 2100 and 2400, causing an increase and decrease respectively in ocean sink magnitude.

4 Discussion

We have used a simple carbon cycle-climate model to investigate the interactions between a selection of idealised CO_2 emissions mitigation trajectories, carbon dioxide removal (CDR), and solar radiation management (SRM) scenarios (Table 2, Figure 3). Most notably, the reduction in temperature caused by implementing SRM also causes a significant reduction in atmospheric CO_2 (Figure 5b). This is due to increased carbon storage by the terrestrial biosphere especially in soils, which only lasts whilst the SRM intervention is in place (Figures 5 & 6). The key mechanism at play in our model is the temperature dependence of soil respiration; cooling by SRM reduces the respiratory losses of carbon from the soil (whilst high CO_2 helps maintain high carbon input to soil via litter fall) (Figure 6). A similar result has been found by others working with more complex models (Matthews & Caldeira, 2007; Matthews *et al.*, 2009). Application of CDR interventions lowers the peak and long term atmospheric CO_2 concentration and global temperature change, and when the CDR ceases the reductions are maintained (Figure 7). When CDR and SRM are implemented together, the impacts on atmospheric CO_2 and global temperature are additive, i.e. the application of CDR reduces the peak and long term atmospheric CO_2 concentration, with a temporary ≈15 ppm further reduction of atmospheric CO_2 whilst SRM is applied (2100 to 2400) (Figure 9). Furthermore, the amount of SRM intervention required to eliminate global warming is less than in the SRM-only case because of the lowered atmospheric CO_2 caused by the CDR (Figure 9c). This synergistic interaction suggests that, at least in this simple formulation, there may be benefits of applying both forms of geoengineering at the same time.

4.1 Interactions with natural carbon sinks

An extensive range of modelling work has focussed on the feedbacks between the climate system and the carbon cycle, whereby increasing atmospheric CO_2 concentration and global temperatures alter the land and ocean carbon sinks (Cox *et al.*, 2000; Friedlingstein *et al.*, 2006; Le Quere *et al.*, 2009). The idealised application of SRM used here and elsewhere creates a modelled future without increased global mean surface temperatures but with elevated atmospheric CO_2 concentrations and in these models this increases both ocean and especially land carbon storage (Matthews & Caldeira, 2007; Matthews *et al.*, 2009). CDR on the other hand, if deployed on a sufficiently large scale, can lower atmospheric CO_2 and global warming, weakening the natural carbon sinks, and potentially turning them into carbon sources. This can be thought of simply as the opposite response to the one observed at present; if rising CO_2 and temperature are causing the land and ocean to increase their carbon storage, then lowering CO_2 and temperature will cause them to lose carbon.

In detail, the results (Figures 6, 8 & 10) are due to the effects of the temperature dependence of photosynthesis, plant respiration, soil respiration and ocean CO_2 solubility; the atmospheric CO_2 concentration dependence of photosynthesis and ocean CO_2 solubility; and the fact that there are lags in the dynamical response of the system. Matthews & Caldeira (2007) used a more complicated Earth system model which encompasses these feedbacks and interactions but with different formulations, and they also found an enhancement of the combined land and ocean sinks when SRM is applied, and that this increased

carbon storage only persists whilst the SRM intervention is in place. Matthews *et al*. (2009) investigated the effects of SRM on ocean acidification and found the land sink to be the dominant cause of the lower atmospheric CO_2 concentration when SRM is applied. Matthews *et al* (2009) applied SRM in 2010 and ran their model until 2100 under the A2 SRES emissions scenario and found in 2100 a 10% increase in land carbon storage in the SRM compared to non-SRM model runs. Our results are not directly comparable (we have a lower emission scenario, see Figure 4, and start SRM later) but have a 3% increase in land carbon storage in 2100 in s2030srm2015 compared to s2030.

To further place our results in context, we can compare our results to what would be expected from the range of 11 models in the C^4MIP inter-comparison (Friedlingstein *et al.*, 2006). Our simple model has a carbon cycle-climate positive feedback gain of g ~ 0.15, which matches the average of the C^4MIP models (range g = 0.04–0.31). A simple relationship can be derived for the effect of SRM on atmospheric CO_2 assuming it returns temperatures to a pre-industrial level (and can therefore be likened to an 'uncoupled' run in the C^4MIP experiments): $\Delta C_A^{SRM} = -g\ \Delta C_A$ where ΔC_A is the increase in atmospheric CO_2 above pre-industrial in the absence of SRM. As an example, in our s2030 scenario ΔC_A = +349 ppm at 2100 and the effect of applying SRM is a drawdown of ΔC_A^{SRM} = –46 ppm in our simple model, whereas the range of C^4MIP models would give ΔC_A^{SRM} = –14 to –108 ppm. Thus, the qualitative result that SRM should reduce atmospheric CO_2 is robust, but the magnitude of the effect ranges over nearly an order of magnitude between models.

Estimates of the land carbon uptake due to SRM varies even more widely between the C^4MIP models over 15–270 PgC in 2100 for applying SRM to the s2030 scenario, whereas in our simple model it is 60 PgC in 2100. Furthermore, our simple model includes interactive land-use change whereas the C^4MIP models do not, and this suppresses land carbon storage prior to 2100, but re-growth combined with CO_2 fertilisation then allows a significant increase in land carbon storage under SRM after 2100.

4.2 Interaction with emissions mitigation

Our results show that commencing emissions reduction activity sooner is more effective at reducing atmospheric CO_2 concentrations than delaying and then implementing carbon dioxide removal (Figures 5b, 7b & 9b). Thus, delaying the start of mitigation activity (T_s) could be very costly in terms of the CDR activity needed later to limit atmospheric CO_2 concentration and corresponding global warming (to a given level). Roughly speaking, in our scenarios, a 15 year delay in the start of mitigation action (from 2015 to 2030) demands ≈300 PgC of CDR over the next two centuries (Figure 7). For reference, historical deforestation has released around 170 PgC (Houghton, 2008). Of course this result is related to our input assumptions, especially the fact that emissions are currently growing exponentially (at a conservative 1.7 % yr^{-1}). Allowing this exponential growth to continue makes a big difference to peak emissions (in s2015, emissions peak in 2033 at 12.3 PgC yr^{-1} whereas in s2030, emissions peak in 2049 at 15.4 PgC yr^{-1}) and hence to cumulative emissions (e.g. cumulative emissions from 2005 to 2100 are 816 PgC for s2015 and 1096 PgC for s2030) (Figure 3a), and therefore atmospheric CO_2 and global temperature change.

Peak global warming has been shown to be well correlated to cumulative anthropogenic carbon emissions (Matthews *et al.*, 2009; Allen *et al.*, 2009), and a cumulative budget of 1000 PgC is estimated to equate to a peak in temperature change of 2 °C (Allen *et al.* 2009). Carbon dioxide removal can be viewed as an

'extreme' form of mitigation whereby the cumulative anthropogenic carbon emissions are reduced. Therefore, if emissions are projected to exceed 1000 PgC (e.g. following a smooth trajectory as in Figure 3a), and the policy aim is to restrict global warming to 2 °C, then CDR could be used to compensate for the overshoot of the budget (Lenton, 2010). However, this is subject to the constraints that CDR can be developed fast enough, deployed on a sufficient scale, and could store enough carbon to avoid transgressing 1000 PgC cumulative loading in the atmosphere-ocean-land system.

In the long term, both the quantity of recoverable fossil fuels and the CO_2 storage capacity need to be critically evaluated and compared. Modelling experiments that assume a quadrupling of CO_2 (e.g. Govindasamy *et al.*, 2003; Lunt *et al.*, 2008, Irvine *et al.*, 2010) require an amount of fossil fuel that well exceeds 'reserves' (economically recoverable). Coal accounts for the largest fraction of fossil fuel reserves. Since 2006, coal has been the largest source of CO_2 from fossil fuel combustion. However, estimates of proved recoverable coal reserves have decreased by 16 % from 2001 to 2009 (World Energy Council, 2001; World Energy Council, 2009). Meanwhile worldwide estimates of the capacity offered by the saline aquifers for the storage of CO_2 are being 'substantially downgraded' (Haszeldine, 2009). Potentially, some methods of mitigation and CDR will compete directly for CO_2 storage capacity. In particular, our bio-energy with carbon storage (BECS) scenario would be making use of the same CO_2 storage capacity as mitigation strategies such as coal power with carbon capture and storage.

SRM can be effective at reducing global temperatures, but if the intervention stops, temperatures rapidly return to the level determined by the atmospheric CO_2 concentration (Matthews & Caldeira, 2007). To avoid this rapid temperature increase, in our model runs, requires maintaining SRM beyond the year 3000 (Figure 5). If the aim however was only to prevent temperatures exceeding a certain level, e.g. 2 °C, then if the profile of atmospheric CO_2 concentration has a peak, as our mitigation scenarios have (Figure 5a), a shorter interval of SRM would suffice. In both of our mitigation scenarios, the canonical 2 °C temperature change is exceeded (for s2015 from 2049 to 2430, for s2030 from 2046 to 3000). Had we chosen to implement SRM to prevent temperatures exceeding 2°C for the s2015 case, this would have required four hundred years of intervention.

4.3 Limitations

There are a number of limitations to these results. We have used a simple representation of carbon cycle-climate feedbacks (Figure 1) (Lenton, 2000). In a spatial model, one can expect the same feedbacks to have a somewhat different strength. Still, the main result, that SRM increases carbon storage has been found in a different, spatial modelling study (Matthews & Caldeira, 2007; Matthews *et al.*, 2009). We do not simulate the direct effects of changes in solar flux on primary production, however previous modelling work has suggested that photosynthesis and plant respiration are relatively insensitive to small reductions in sunlight (Govindasamy *et al.,* 2002). Furthermore, changes in solar flux and atmospheric CO_2 may be considered independent in terms of their effect on NPP.

Other processes not included here may further change the magnitude and perhaps the direction, of the results. For example, the CO_2 fertilisation effect is not constrained by nutrient limitation. Furthermore, several modelling studies have shown that SRM interventions cause global and regionally disparate changes to precipitation (Bala *et al.*, 2008; Ricke *et al.*, 2009; Irvine *et al.*, 2010). These changes to precipitation may in turn alter carbon storage, and impact on the viability of afforestation in certain regions. We do not

assess the impact of afforestation on albedo, or on emissions of volatile organic carbon compounds, with attendant effects on atmospheric chemistry and cloud micro-physics. Indeed, we have excluded all non-CO_2 anthropogenic radiative forcing agents such as methane, nitrous oxide, ozone, or aerosols.

We have not explicitly defined a mechanism of SRM here and there are a number of possibilities, with differing implications and potential feedbacks within the climate system (Vaughan & Lenton, 2011). In particular, the use of stratospheric sulphate aerosols would increase the diffuse fraction of incoming solar radiation, which may increase photosynthetic efficiency (Rasch *et al.*, 2008). Our method of back-calculating the amount of SRM required to maintain pre-industrial temperatures (Figures 3c & 9c), hides a considerable challenge for any choice of SRM method; that of continually modifying its magnitude. Not all suggested SRM methods could achieve this (Vaughan & Lenton, 2011). The challenge is made more difficult if the real Earth system has a relatively high heat capacity, and hence temperature responds more slowly to radiative forcing perturbations. Our model has a relatively rapid temperature response i.e. a small heat capacity, but elsewhere (Vaughan *et al.*, 2009) we present a sensitivity analysis to varying the model heat capacity.

Despite the inevitable limitations of working with a simple model, the results obtained offer a provocation to consider the interactions between mitigation, CDR and SRM in more comprehensive models.

5. Conclusion

Avoiding a 15 year delay in the start of mitigation activity is more effective at reducing atmospheric CO_2 concentrations than all but the maximum type of carbon dioxide removal interventions. Mitigation trajectories determine both the magnitude of CDR and/or the magnitude and duration of SRM intervention required to avoid any particular threshold or target of atmospheric CO_2 concentration or mean global temperature change. In our model, the effects of applying SRM and CDR together are additive, and this shows most clearly for atmospheric CO_2 concentration. SRM causes a significant reduction in atmospheric CO_2 concentration due to increased carbon storage by the terrestrial biosphere, especially in soils. However, SRM still has to be maintained for many centuries to avoid rapid increases in temperature and corresponding increases in atmospheric CO_2 concentration, due to loss of carbon from the land. From a cumulative emissions perspective, there is a clear top-down trade-off between mitigation and CDR, whereby CDR can be considered ‘extreme’ mitigation. We have not addressed the mechanism by which CDR or SRM is achieved in any detail, but from a bottom-up level there are many more potential interactions between CDR and mitigation. These interactions, between technologies, land use and land availability, water resources availability and CO_2 storage capacity could include both synergistic and antagonistic ones. Together, the trajectory of future CO_2 emissions, the capacity of CDR, and the land and ocean sink response, will determine the magnitude, duration and need for any SRM interventions.

Vaughan, N. E. & Lenton, T. M. (2012) Interactions between reducing CO_2 emissions, CO_2 removal and solar radiation management ***Phil. Trans. R. Soc. A*** **370**(1974):4343-4364 **doi: 10.1098/rsta.2012.0188** Published 6 August 2012 **http://rsta.royalsocietypublishing.org/content/370/1974/4343**

Acknowledgements

NEV is funded by the Tyndall Centre for Climate Change Research and the EPSRC project Integrated Assessment of Geoengineering Proposals (IAGP) (EP/I014721/1). This work was also supported by the Norfolk Charitable Trust through the GeoEngineering Assessment & Research (GEAR) initiative. TML thanks NERC (NE/G018332/1) for support.

References

Allen, M.R., Frame, D.J., Huntingford, C., Jones, C.D., Lowe, J.A., Meinshausen, M. & Meinshausen, N. 2009 Warming caused by cumulative carbon emissions towards the trillionth tonne. *Nature* **458,** 1163-1166. (DOI: 10.1038/nature08019).

Anderson, K. & Bows, A. 2008 Reframing the climate change challenge in light of post-2000 emission trends. *Phil Trans R Soc A* **366**, 3863-3882 (DOI:10.1098/rsta.2008.0138).

Bala, G., Duffy, P. B. & Taylor, K. E. 2008 Impact of geoengineering schemes on the global hydrological cycle. *PNAS* **105**, 7664-7669 (DOI:10.1073/pnas.0711648105).

Boden, T. A., Marland, G. & Andres, R. J. 2011 Global, Regional, and National Fossil-Fuel CO_2 emissions. *Carbon Dioxide Information Analysis Center, Oak Ridge National Laboratory, U.S. Department of Energy, Oak Ridge, Tenn. U.S.A.* (DOI: 10.3334/CDIAC/00001_V2011).

Boden, T. A. & Blasing, T.J. 2011 Preliminary 2009 & 2010 Global & National Estimates by Extrapolation. See http://cdiac.ornl.gov/trends/emis/perlim_2009_2010_estimates.html

Caldeira, K. & Wood, L. 2008 Global and Arctic climate engineering: numerical model studies. *Phil Trans R Soc A* **366**, 4039-4056 (DOI:10.1098/rsta.2008.0132).

Conway, T.J. & Tans, P.P. 2011 National Oceanic and Atmospheric Administration/Earth System Research Laboratory. See www.esrl.noaa.gov/gmd/ccgg/trends/

Conway, T. J., Tans, P.P. , Waterman, L.S., Thoning, K.W., Kitzis, D., Masarie, K. A. & Zhang, N. 1994 Evidence for interannual variability of the carbon cycle from the National Oceanic and Atmospheric Administration/Climate Monitoring and Diagnostics Laboratory Global Air Sampling Network. *Journal of Geophysical Research-Atmospheres.* **99**, 22831-22855 (DOI: 10.1029/94JD01951).

Cox, P. M., Betts, R. A., Jones, C. D., Spall, S. A. & Totterdell, I. J. 2000 Acceleration of global warming due to carbon-cycle feedbacks in a coupled climate model. *Nature* **408**, 184-187 (DOI: 10.1038/35041539).

Crutzen, P. J. 2006 Albedo enhancement by stratospheric sulphur injections: a contribution to resolve a policy dilemma? *Climatic Change* **77**, 211-219 (DOI: 10.1007/s10584-006-9101-y).

Etheridge, D.M., Steele, L.P., Langenfelds, R.L., Francey, R.J., Barnola, J.-M. & Morgan, V.I. 1998 Historical CO_2 records from the Law Dome DE08, DE08-2, and DSS ice cores. In *TRENDS: A Compendium of Data on Global Change*. Carbon Dioxide Information Analysis Center, U.S. Department of Energy.

Friedlingstein, P., Cox, P., Betts, R., Bopp, L., von Bloh, W., Brovkin, V., Cadule, P., Doney, S., Eby, M., Fung, I., *et al* 2006 Climate-Carbon Cycle Feedback Analysis: Results from the C^4MIP Model Intercomparison. *Journal of Climate* **19**, 3337-3353 (DOI: 10.1175/JCLI3800.1).

Govindasamy, B. & Caldeira, K. 2000 Geoengineering Earth's radiation balance to mitigate CO_2-induced climate change. *Geophysical Research Letters* **27**, 2142-2144 (DOI: 10.1029/1999GL006086).

Govindasamy, B., Caldeira, K. & Duffy, P. B. 2003 Geoengineering Earth's radiation balance to mitigate climate change from a quadrupling of CO_2. *Global and Planetary Change* **37**, 157-168 (DOI: 10.1016/S0921-8181(02)00195-9).

Govindasamy, B., Thompson, S., Duffy, P. B., Caldeira, K. & Delire, C. 2002 Impact of geoengineering schemes on the terrestrial biosphere. *Geophysical Research Letters* **29**, 2061 (DOI:10.10290/2002GL015911).

Haszeldine, R. S. 2009 Carbon capture and storage: how green can black be? *Science* **325**, 1647-1652 (DOI:10.1126/science.1172246).

Houghton, R. A. 2008 Carbon Flux to the Atmosphere from Land-Use Changes: 1850-2005. In *TRENDS: A Compendium of Data on Global Change.* Carbon Dioxide Information Analysis Center, Oak Ridge National Laboratory, U.S. Department of Energy, Oak Ridge, Tenn. U.S.A.

Irvine, P. J., Ridgwell, A. & Lunt, D. J. 2010 Assessing the regional disparities in geoengineering impacts. *Geophysical Research Letters* **37**, L18702 (DOI:10.1029/2010GL044447).

Lenton, T. M. 2000 Land and ocean carbon cycle feedback effects on global warming in a simple Earth system model. *Tellus B* **52**, 1159-1188 (DOI: 10.1034/j.1600-0889.2000.01104.x).

Lenton, T. M. 2010 The potential for land-based biological CO_2 removal to lower future atmospheric CO_2 concentration. *Carbon Management* **1**, 1-16 (DOI: 10.4155/CMT.10.12).

Lenton, T. M. & Huntingford, C. 2003 Global terrestrial carbon storage and uncertainties in its temperature sensitivity examined with a simple model. *Global Change Biology* **9**, 1333-1352 (DOI: 10.1046/j.1365-2486.2003.00674.x).

Lenton, T. M. & Vaughan, N. E. 2009 The radiative forcing potential of different climate geoengineering options. *Atmospheric Chemistry & Physics* **9**, 5539-5561 (DOI: 10.5194/acpd-9-2559-2009).

Le Quere, C., Raupach, M. R., Canadell, J. G., Marland, G., Bopp, L., Ciais, P., Conway, T. J., Doney, S. C., Feely, R. A., Foster, P., *et al* 2009 Trends in the sources and sinks of carbon dioxide. *Nature Geoscience* **2**, 831-836 (DOI:10.1038/NGEO689).

Lunt, D. J., Ridgwell, A., Valdes, P. J. & Seale, A. 2008 "Sunshade world": a fully coupled GCM evaluation of the climate impacts of geoengineering. *Geophysical Research Letters* **35**, L12710 (DOI: 10.1029/2008GL033674).

Matthews, H. D. & Caldeira, K. 2007 Transient climate-carbon simulations of planetary geoengineering. *PNAS* **104**, 9949-9954 (DOI:10.1073/pnas.0700419104).

Matthews, H. D., Cao, L. & Caldeira, K. 2009 Sensitivity of ocean acidification to geoengineering climate stabilization. *Geophysical Research Letters* **36,** L10706 (DOI: 10.1029/2009GL037488).

Matthews, H. D., Gillett, N. P., Stott, P. A. & Zickfeld, K. 2009 The proportionality of global warming to cumulative carbon emissions. *Nature* **459**, 829-832 (DOI: 10.1038/nature08047).

Meinshausen, M., Smith, S.J., Calvin, K., Daniel, J.S., Kainuma, M.L.T., Lamarque, J.-F., Matsumo, K., Montzka, S.A., Raper, S.C.B., Riahi, K., Thomson, A., Velders, G.J.M. & van Vuuren, D.P.P. 2011 The RCP greenhouse gas concentrations and their extensions from 1765 to 2300. *Climatic Change* **109**, 213-241 (DOI:10.1007/s10584-011-0156-z).

Moore, J. C., Jevrejeva, S. & Grinsted, A. 2010 Efficacy of geoengineering to limit 21st century sea-level rise. *PNAS* **107**, 15699-15703 (DOI: 10.1073/pnas.1008153107).

Moss, R. H., Edmonds, J. A., Hibbard, K. A., Manning, M. R., Rose, S. K., van Vuuren, D. P., Carter, T. R., Emori, S., Kainuma, M., Kram, T., *et al* 2010 The next generation of scenarios for climate change research and assessment. *Nature* **463**, 747-756 (DOI: 10.1038/nature08823).

Nakicenovic, N. & Swart, R. (Eds.) 2000 *Special Report on Emission Scenarios: A Special Report of Working Group III of the Intergovernmental Panel on Climate Change*. Cambridge University Press.

Vaughan, N. E. & Lenton, T. M. (2012) Interactions between reducing CO_2 emissions, CO_2 removal and solar radiation management ***Phil. Trans. R. Soc. A*** **370**(1974):4343-4364 **doi: 10.1098/rsta.2012.0188** Published 6 August 2012 **http://rsta.royalsocietypublishing.org/content/370/1974/4343**

Neftel, A., Friedli, H., Moor, E., Lötscher, H., Oeschger, H., Siegenthaler, U. & Stauffer, B. 1994 Historical CO_2 record from the Siple Station ice core. In *TRENDS: A Compendium of Data on Global Change.* Carbon Dioxide Information Analysis Center, U.S. Department of Energy.

Rasch, P. J., Tilmes, S., Turco, R. P., Robock, A., Oman, L., Chen, C-C, Stenchikov, G. L. & Garcia, R. R. (2008) An overview of geoengineering of climate using stratospheric sulphate aerosols. *Phil Trans R Soc A* **366**, 4007-4037 (DOI:10.1098/rsta.2008.0131).

Ricke, K. L., Granger Morgan, M. & Allen, M. R. 2009 Regional climate response to solar radiation management. *Nature Geoscience* **3**, 537-541 (DOI: 10.1038/NGE0915).

The Royal Society 2009 *Geoengineering the climate. Science, governance and uncertainty.* London: The Royal Society.

United Nations Population Division 1999 *The World at Six Billion.* Document ESA/P/WP.154 12 October 1999. New York: United Nations.

van Minnen, J.G., Strengers, B.J., Eickhout, E., Swart, R.J. & Leemans, R. 2008 Quantifying the effectiveness of climate change mitigation through forest plantation and carbon sequestration with an integrated land-use model. *Carbon Balance and Management* **3,** 3 (DOI: doi:10.1186/1750-0680-3-3).

van Vuuren, D.P., Edmonds, J., Kainuma, M., Riahi, K., Thomson, A., Hibbard, K., Hurtt, G.C., Kram, T., Krey, V., Lamarque, J.-F., Masui, T., Meinshausen, M., Nakicenovic, N., Smith, S.J. & Rose, S.K. 2011 The representative concentration pathways: an overview. *Climatic Change* **109**, 5-31 (DOI: 10.1007/s10584-011-0148-z).

Vaughan, N. E., Lenton, T. M. & Shepherd, J. S. 2009 Climate change mitigation: trade-offs between delay and strength of action required. *Climatic Change* **96**, 29-43 (DOI: 10.1007/s10584-009-9573-7).

Vaughan, N. E. and Lenton, T. M. 2011 A review of climate geoengineering proposals. *Climatic Change* **109**, 749-790 (DOI: 10.1007/s10584-011-0027-7).

Wigley, T. M. L. 2006 A combined mitigation/geoengineering approach to climate stabilization *Science* **314**, 452-454 (DOI: 10.1126/science.1131728).

World Energy Council 2001 *Survey of Energy Resources 2001,* 19th edn. London: World Energy Council.

World Energy Council 2009 *Survey of Energy Resources Interim Update 2009.* London: World Energy Council.

Vaughan, N. E. & Lenton, T. M. (2012) Interactions between reducing CO_2 emissions, CO_2 removal and solar radiation management ***Phil. Trans. R. Soc. A*** **370**(1974):4343-4364 **doi: 10.1098/rsta.2012.0188** Published 6 August 2012 **http://rsta.royalsocietypublishing.org/content/370/1974/4343**

Figures

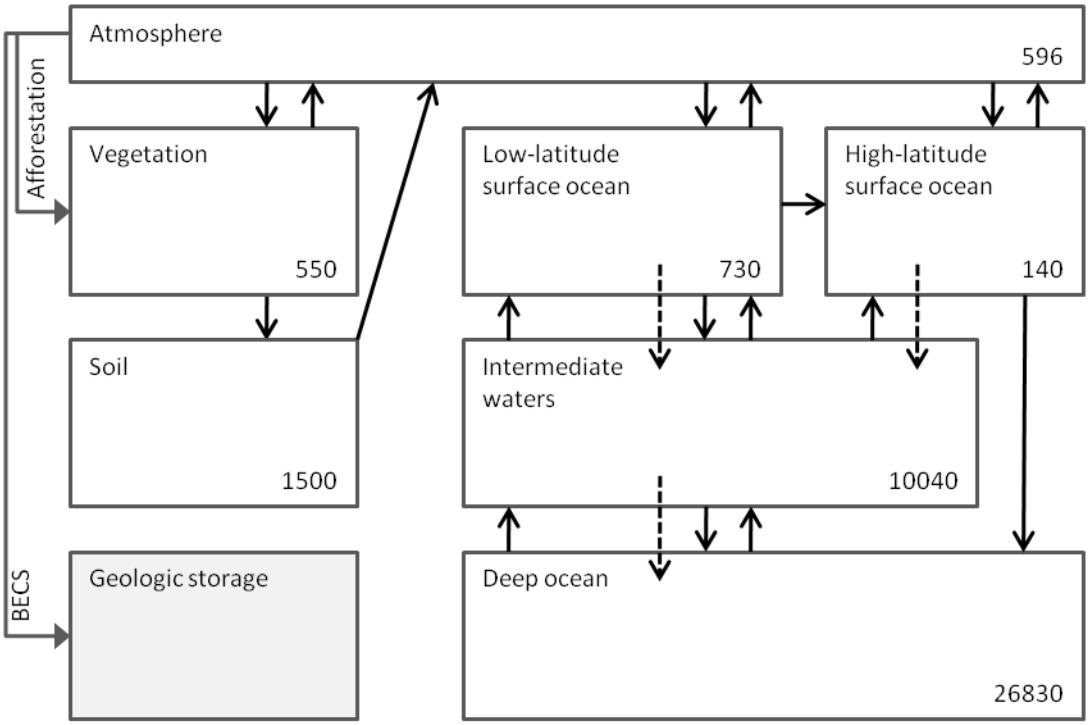

Figure 1 Schematic of carbon cycle box model with CDR interventions. Pre-industrial steady state carbon cycle, with reservoir sizes in petagrams of carbon (PgC) and fluxes of carbon indicated by arrows. For the ocean boxes, solid arrows are flows of water, dashed arrows are sinking particulate fluxes. Flux sizes are detailed in Lenton (2000). The two CDR interventions, afforestation and BECS are illustrated.

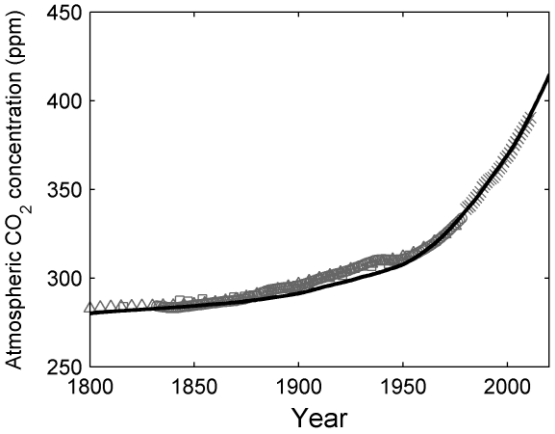

Figure 2 Atmospheric CO_2 concentration from 1800 to 2010 generated by the simple carbon cycle-climate model (solid black line) (Lenton,2000) and compared to atmospheric CO_2 concentration data from Siple ice core (grey squares) (Neftel *et al.*, 1994), Law Dome ice core data with a 20-year cut off spline smoothing (grey circles) and a 75-year cut off spline smoothing (grey triangles) (Etheridge *et al.,* 1998), and direct atmospheric measurements of globally averaged marine surface atmospheric CO_2 (grey crosses) (Conway et al., 1994; Conway & Tan 2011).

Vaughan, N. E. & Lenton, T. M. (2012) Interactions between reducing CO_2 emissions, CO_2 removal and solar radiation management ***Phil. Trans. R. Soc. A*** **370**(1974):4343-4364 **doi: 10.1098/rsta.2012.0188** Published 6 August 2012 **http://rsta.royalsocietypublishing.org/content/370/1974/4343**

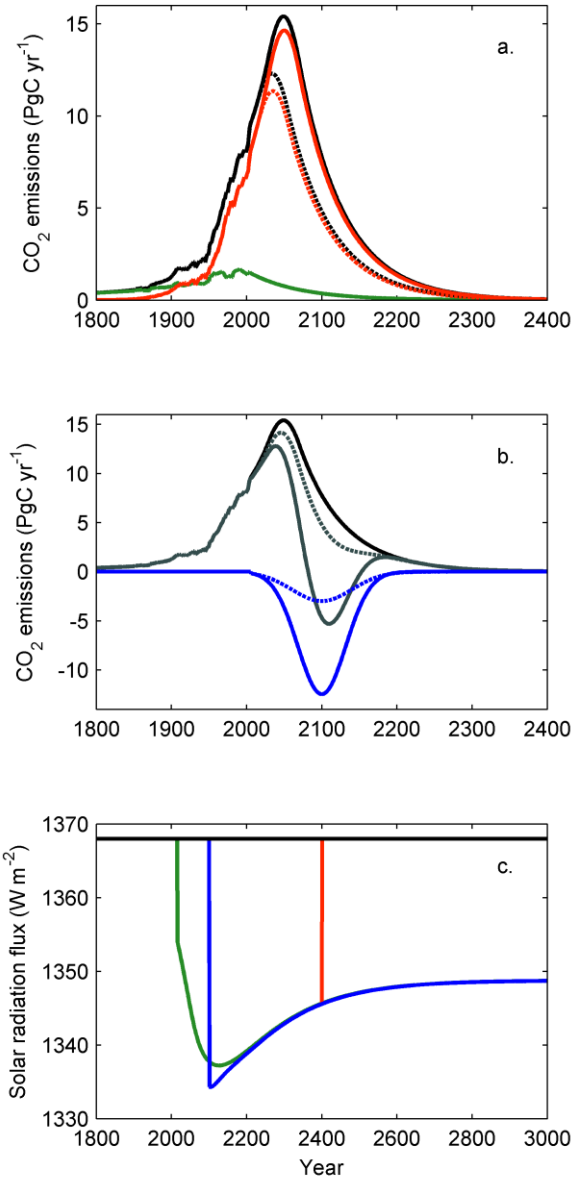

Figure 3 Model forcing comprising of (a) anthropogenic CO_2 emissions, (b) CDR interventions and (c) SRM interventions. (a) Net anthropogenic CO_2 emissions (black) consist of land use change emissions (green) and emissions from fossil fuel combustion and cement production (red). Two mitigation scenarios are illustrated, s2015 (dashed) and s2030 (solid). (b) Carbon dioxide removal (CDR) scenarios afforestation (blue dashed) and BECS (blue solid). Net anthropogenic emissions for mitigation scenario s2030 with no CDR (black), afforestation (grey dashed), and BECS (grey solid). (c) Changes to solar radiation flux caused by solar radiation modification (SRM) in which the atmospheric CO_2 perturbation is counteracted entirely, for the following durations; none (black), starting in 2015 (green), starting in 2100 (blue), starting in 2100 and ceasing in 2400 (red).

Vaughan, N. E. & Lenton, T. M. (2012) Interactions between reducing CO_2 emissions, CO_2 removal and solar radiation management ***Phil. Trans. R. Soc. A*** **370**(1974):4343-4364 **doi: 10.1098/rsta.2012.0188** Published 6 August 2012 **http://rsta.royalsocietypublishing.org/content/370/1974/4343**

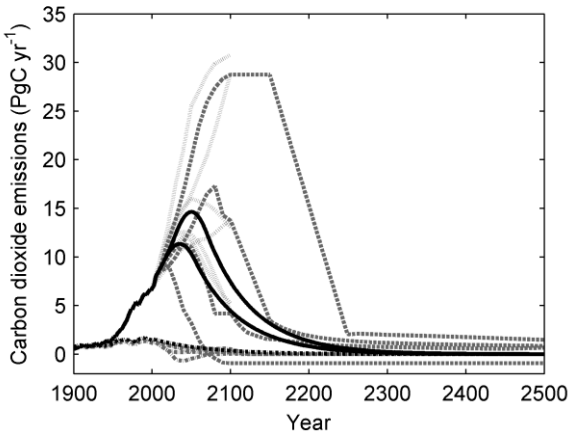

Figure 4 Comparison of existing carbon dioxide emission scenarios with the emission scenarios used in the model for fossil fuel combustion and cement production (solid black lines) and land-use change (dotted-dashed black line). Historical data are used from 1800 to 2005 (Houghton, 2008; Boden *et al*., 2011) and future scenarios, one for land-use change and two for fossil fuel combustion and cement production (s2015 and s2030). Are constructed for 2005-3000 (see Section 2). For comparison, the Special Report on Emissions Scenarios (SRES) fossil fuel combustion and cement production marker scenarios (A1B, A1FI, A1T, B1, A2, B2; light grey dotted) (Nakicenovic & Swart, 2000) and the emission scenarios used to create the Representative Concentration Pathways (RCP3PD, RCP4.5, RCP6, RCP8) (Moss *et al.*, 2010; van Vuuren *et al.*, 2011; Meinshausen *et al.*, 2011) for land-use change (dotted-dashed grey) and fossil fuel combustion and cement production (dashed grey) are shown. Note the SRES scenarios are from 1990 to 2100; the RCP scenarios are from 2000-2100; with extensions out to 2500.

Vaughan, N. E. & Lenton, T. M. (2012) Interactions between reducing CO_2 emissions, CO_2 removal and solar radiation management ***Phil. Trans. R. Soc. A*** **370**(1974):4343-4364 **doi: 10.1098/rsta.2012.0188** Published 6 August 2012 **http://rsta.royalsocietypublishing.org/content/370/1974/4343**

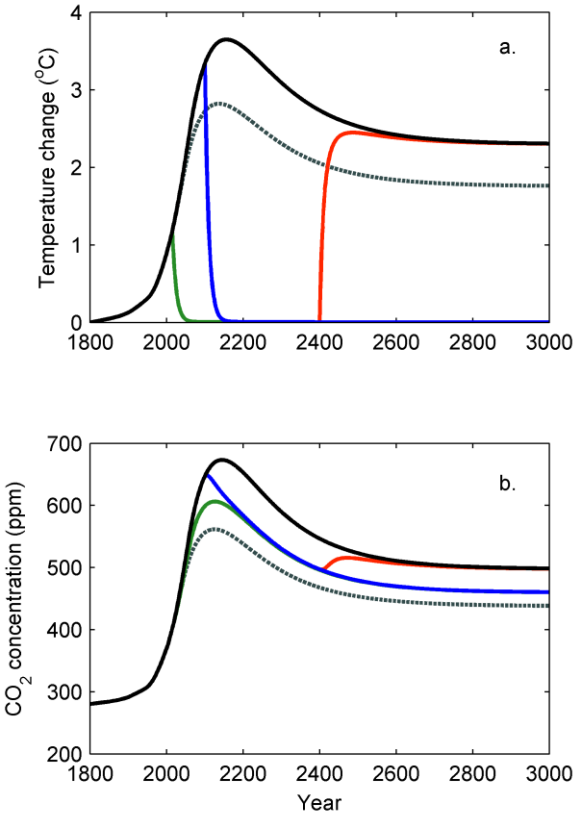

Figure 5 Impact of SRM interventions on (a) global temperature change and (b) atmospheric CO_2 concentration. Mitigation scenario s2030 (black) and s2015 (grey dashed) with no SRM intervention. Mitigation scenario s2030 with SRM intervention starting in 2015 (green), 2100 (blue) and starting in 2100 and ceasing in 2400 (red solid).

Vaughan, N. E. & Lenton, T. M. (2012) Interactions between reducing CO_2 emissions, CO_2 removal and solar radiation management ***Phil. Trans. R. Soc. A*** **370**(1974):4343-4364 **doi: 10.1098/rsta.2012.0188** Published 6 August 2012 **http://rsta.royalsocietypublishing.org/content/370/1974/4343**

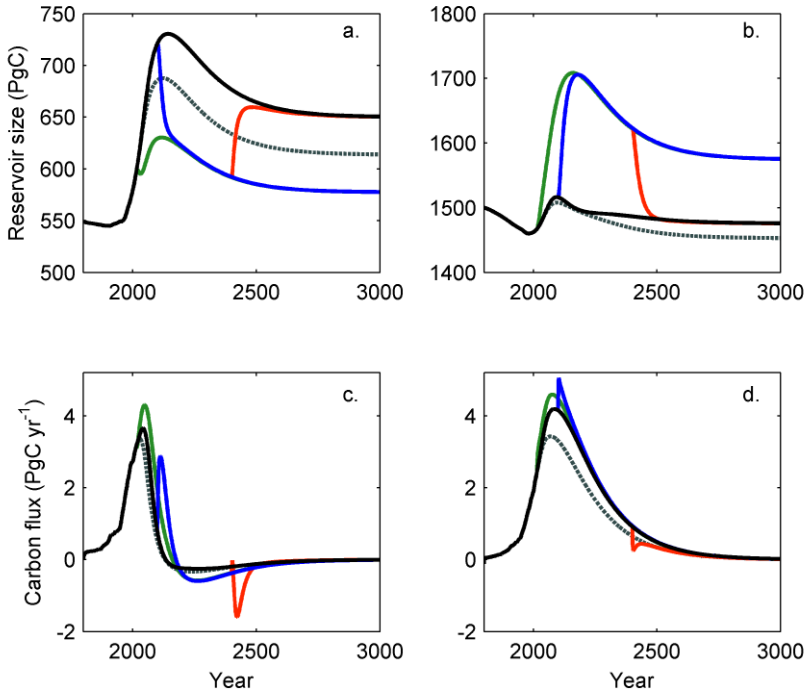

Figure 6 Impact of SRM interventions on (a) vegetation carbon reservoir, (b) soil carbon reservoir, (c) land carbon sink and (d) ocean carbon sink. Mitigation scenario s2030 (black) and s2015 (grey dashed) with no SRM intervention. Mitigation scenario s2030 with SRM intervention starting in 2015 (green), 2100 (blue) and starting in 2100 and ceasing in 2400 (red). Note the difference in y-axis scale between (a) and (b). Note (c) and (d) are carbon sinks; positive values are a removal of carbon from the atmosphere and negative values are an addition of carbon to the atmosphere.

Vaughan, N. E. & Lenton, T. M. (2012) Interactions between reducing CO_2 emissions, CO_2 removal and solar radiation management ***Phil. Trans. R. Soc. A*** **370**(1974):4343-4364 **doi: 10.1098/rsta.2012.0188** Published 6 August 2012 **http://rsta.royalsocietypublishing.org/content/370/1974/4343**

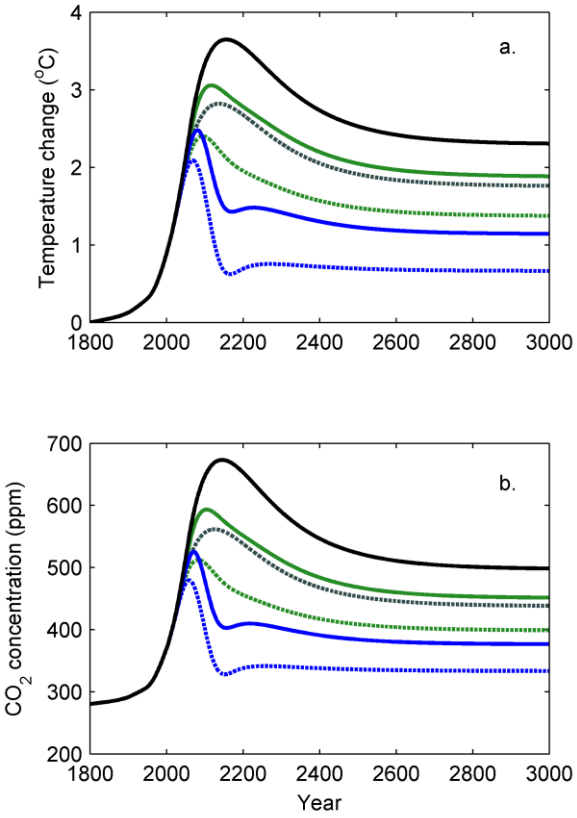

Figure 7 Impact of CDR interventions on (a) global temperature change and (b) atmospheric CO_2 concentration. Mitigation scenario s2030 with no CDR (black), afforestation (green solid) and BECS (blue solid). Mitigation scenario s2015 with no CDR (grey dashed), afforestation (green dashed) and BECS (blue dashed).

Vaughan, N. E. & Lenton, T. M. (2012) Interactions between reducing CO_2 emissions, CO_2 removal and solar radiation management ***Phil. Trans. R. Soc. A*** **370**(1974):4343-4364 **doi: 10.1098/rsta.2012.0188** Published 6 August 2012 **http://rsta.royalsocietypublishing.org/content/370/1974/4343**

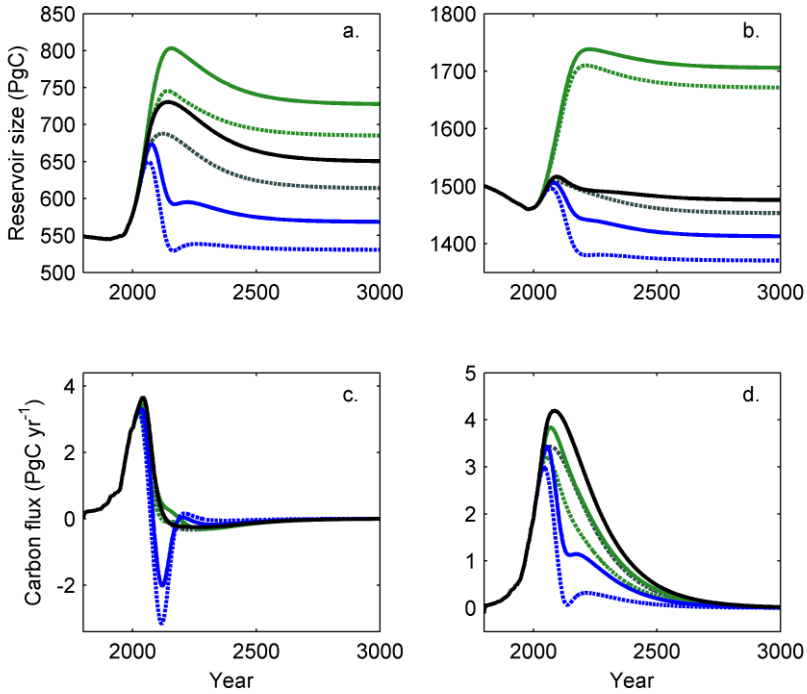

Figure 8 Impact of CDR interventions on (a) vegetation carbon reservoir, (b) soil carbon reservoir, (c) land carbon sink and (d) ocean carbon sink. Mitigation scenario s2030 with no CDR (black), afforestation (green solid) and BECS (blue solid). Mitigation scenario s2015 with no CDR (grey dashed), afforestation (green dashed) and BECS (blue dashed). Note the difference in y-axis scale between (a) and (b). Note (c) and (d) are carbon sinks; positive values are a removal of carbon from the atmosphere and negative values are an addition of carbon to the atmosphere.

Vaughan, N. E. & Lenton, T. M. (2012) Interactions between reducing CO_2 emissions, CO_2 removal and solar radiation management ***Phil. Trans. R. Soc. A*** **370**(1974):4343-4364 **doi: 10.1098/rsta.2012.0188** Published 6 August 2012 **http://rsta.royalsocietypublishing.org/content/370/1974/4343**

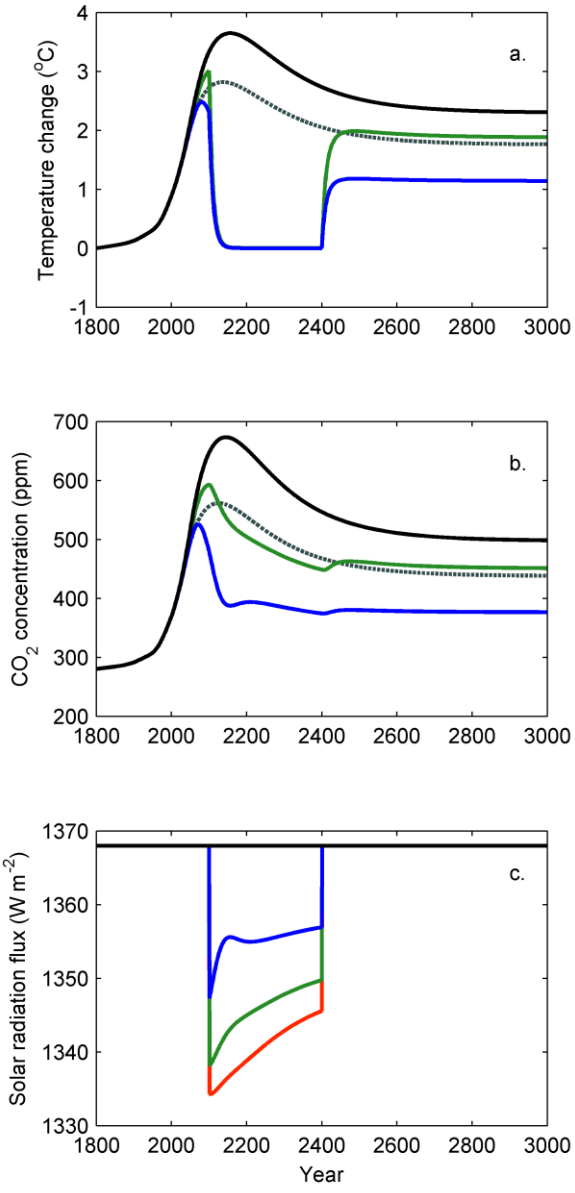

Figure 9 Impact of combinations of SRM and CDR interventions on (a) global temperature change, (b) atmospheric CO_2 concentration and (c) magnitude of SRM intervention. No SRM or CDR intervention with mitigation scenario s2030 (black) and s2015 (grey dashed). Mitigation scenario s2030 and SRM intervention starting in 2100 and ceasing in 2400 (red), with CDR intervention afforestation (green) and with CDR intervention BECS (blue). Note the s2030srm21002400 (red) is only shown in panel (c) to show the impact of the combined interventions on the magnitude of SRM required. For global temperature change and atmospheric CO_2 concentration for s2030srm21002400 see Figure 3.

Vaughan, N. E. & Lenton, T. M. (2012) Interactions between reducing CO_2 emissions, CO_2 removal and solar radiation management ***Phil. Trans. R. Soc. A*** **370**(1974):4343-4364 **doi: 10.1098/rsta.2012.0188** Published 6 August 2012 **http://rsta.royalsocietypublishing.org/content/370/1974/4343**

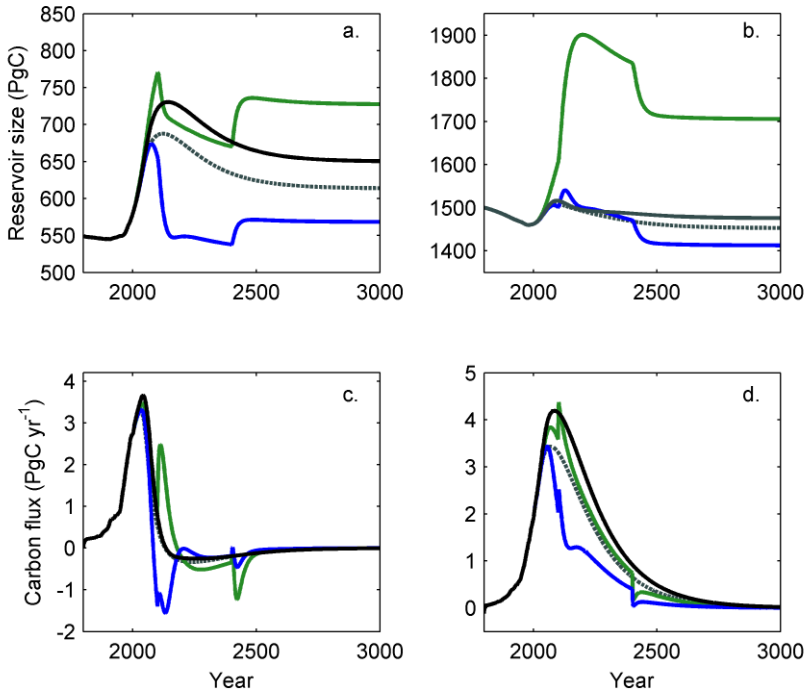

Figure 10 Impact of combinations of SRM and CDR interventions on (a) vegetation carbon reservoir, (b) soil carbon reservoir, (c) land carbon sink and (d) ocean carbon sink. No SRM or CDR intervention with mitigation scenario s2030 (black) and s2015 (grey dashed). Mitigation scenario s2030 with CDR intervention afforestation (green) and with CDR intervention BECS (blue). Note the difference in y-axis scale between (a) and (b). Note (c) and (d) are carbon sinks; positive values are a removal of carbon from the atmosphere and negative values are an addition of carbon to the atmosphere.